Cement & Concrete Composites 30 (2008) 872–879

Contents lists available at ScienceDirect

Cement & Concrete Composites

journal homepage: www.elsevier.com/locate/cemconcomp

Self-healing of mechanically-loaded self consolidating concretes with high volumes of fly ash

Mustafa Şahmaran [a,*], Suleyman B. Keskin [b], Gozde Ozerkan [b], Ismail O. Yaman [b]

[a] Department of Civil Engineering, University of Gaziantep, Gaziantep, Turkey
[b] Department of Civil Engineering, Middle East Technical University, Ankara, Turkey

ARTICLE INFO

Article history:
Received 10 April 2008
Received in revised form 1 July 2008
Accepted 2 July 2008
Available online 10 July 2008

Keywords:
Self consolidating concrete
High volume fly ash
Self-healing
Mechanical and permeation properties

ABSTRACT

This article discusses the effects of self-healing on self consolidating concretes incorporating high volumes of fly ash (HVFA–SCC) when subjected to continuous water exposure. For this purpose, self consolidating concretes with fly ash replacement ratios of 0%, 35%, and 55% were prepared having a constant water-cementitious material ratio of 0.35. A uniaxial compression load was applied to generate microcracks in concrete where cylindrical specimens were pre-loaded up to 70% and 90% of the ultimate compressive load determined at 28 days. Later, the extent of damage was determined as percentage of loss in mechanical properties (as determined by compressive strength and ultrasonic pulse velocity) and percentage of increase in permeation properties (rapid chloride permeability and sorptivity index). After pre-loading, concrete specimens were stored in water for a month and the mechanical and permeation properties are monitored at every two weeks. It was observed that HVFA-SCC mixtures initially lost 27% of their strength when pre-loaded up to 90% of their ultimate strength, and after 30 days of water curing that reduction was only 7%, indicating a substantial healing. On the other hand, for SCC specimens without fly ash that were pre-loaded to the same level, the loss in strength was initially 19%, and after a month of moist curing it was only 13%. Similar observations were also made on the permeation properties with greater effects. As the HVFA-SCCs studied have an important amount of unhydrated fly ash available in their microstructure, these observations are attributed to the self-healing of the pre-existing cracks, mainly by hydration of anhydrous fly ash particles on the crack surfaces.

1. Introduction

Increased durability of reinforced concrete is typically associated with a dense concrete matrix, i.e. a very compact microstructure is expected to lower permeability and reduce the transport of corrosive agents to reinforcement [1,2]. Conceptually, a dense matrix can be achieved by a well-graded particle size distribution [3], by the use of mineral additives such as fly ash and silica fume [4], or by the use of low water-to-cement ratios [5]. These concepts, however, rely upon the concrete to remain uncracked within a structure throughout its expected service life. In this presumed uncracked state, such concretes have proven to be durable in laboratory tests [6,7].

In reality however, cracking in concrete is inevitable. Interfacial microcracks do exist at the aggregate–cement interface and further cracking may occur during the service life of a concrete structure due to external loading, intrinsic volumetric instability or deleterious chemical reactions [8,9]. The durability of concrete is intimately related to its transport properties, particularly with respect to transport of moisture. This is because concrete is susceptible to degradation through leaching, corrosion, sulfate attack, freezing and thawing damage, and other mechanisms that necessitate the ingress of water. Because cracks significantly modify the transport properties of concrete, their presence greatly accelerates the deterioration process.

Self consolidating concrete (SCC), one of the latest achievements of concrete technology, has been, first, introduced by Japanese researchers with an intent to increase the durability of reinforced concrete structures by increasing the workability of concrete and thus by increasing the construction quality [10]. Numerous studies have examined the mechanical and permeation properties of uncracked SCC [11–15]. The permeation of uncracked SCC has been related principally to the particle density of the composite, typically a function of water to cement ratio whose effect was initially stated by the pioneering work of Powers et al. [16]. This relation of low permeability to high density is one of the reasons that self consolidating concretes, with significantly higher particle packing than normal concretes, are considered highly durable. However, SCCs, in comparison to conventional concretes, show much higher levels of thermal and autogenous shrinkage due to the lower water to cement ratio and higher amount of

* Corresponding author. Tel.: +90 342 317 2410; fax: +90 342 360 1107.
E-mail address: sahmaran@umich.edu (M. Şahmaran).

0958-9465/$ - see front matter © 2008 Elsevier Ltd. All rights reserved.
doi:10.1016/j.cemconcomp.2008.07.001

binder content [13]. Together with a high Young's modulus, low creep coefficient and high brittleness, these high strength SCCs are far more likely to crack at an early age than normal strength concretes. Once cracked, the permeability of SCCs, regardless of matrix density or compressive strength, will increase remarkably. It was shown that by the use of fly ash, it is possible to improve the performance of SCCs by reducing its shrinkage and modulus of elasticity [14,15], and making them less vulnerable to cracking. However there is still a need to further investigate the issue of cracking in SCCs.

The effect of self-healing of cracks on permeation and mechanical properties of conventional concrete has been widely investigated by other researchers [17–24]. However, no information is currently available on the self-healing of high volume fly ash SCC (HVFA-SCC) subjected to mechanical loading. Thus, it may be significant to investigate the mechanical and permeation properties of cracked and healed HVFA-SCC. In the present research, experimental work was conducted to explore and investigate the self-healing potential of HVFA-SCCs that are subjected to mechanical loads. For this purpose, two HVFA–SCC mixtures were prepared by keeping the total mass of binder (Portland cement + fly ash) constant at 500 kg/m^3, in which 35% and 55% of binder, by mass, was replaced by a low-lime fly ash. For comparison, a control SCC mixture without fly ash was also produced. The mechanical and permeation properties of pre-loaded SCC specimens were monitored for 30 days. These properties included the compressive strength, ultrasonic pulse velocity, rapid chloride permeability and sorptivity.

2. Experimental program

2.1. Material properties of ingredients

The cement used in all mixtures was a normal Portland cement (PC) CEM I 42.5 R, equivalent to ASTM Type I Portland cement [25]. The low-lime fly ash (FA) with a lime content of 4.24% was used in this study. Chemical composition and physical properties of PC and FA are presented in Table 1. The particle size distributions of these materials were also obtained, by a laser scattering technique and are given in Fig. 1. As for the aggregates, crushed limestone with the maximum aggregate size of 19 mm and crushed sand from the same local source were used. Both the coarse and fine aggregate had a specific gravity of 2.70, and water absorptions of 0.5% and 1.2%, respectively. A polycarboxylic-ether type superplasticizer (SP) (ADVA® Cast 570) with a specific gravity of 1.08, pH of 5.7 and a solid content of 40% was used in all concrete mixtures.

2.2. Mixture proportions, preparation and casting of test specimens

Three concrete mixtures were prepared with the proportions summarized in Table 2. The control mixture included only PC as a binder. Remaining mixtures had FA replacement ratios of 35% and 55%, by mass of binder (PC + FA). For all mixtures, the total amount of binder and the water–binder ratio (W/B), by mass, were kept constant. SP was added to achieve similar slump flow for all mixtures of 650 ± 25 mm; therefore, the SP content was not kept constant.

Table 1
Properties of the Portland cement and fly ash

Chemical composition	Cement	Fly ash
CaO (%)	63.27	4.24
SiO_2 (%)	19.61	56.20
Al_2O_3 (%)	5.86	20.17
Fe_2O_3 (%)	3.40	6.69
MgO (%)	0.95	1.92
SO_3 (%)	2.45	0.49
K_2O (%)	0.54	1.89
Na_2O (%)	0.47	0.58
Loss on ignition (%)	3.02	1.78
Physical properties		
Specific gravity	3.14	2.25
Blaine fineness (m^2/kg)	362.9	287.0

All of the concrete mixtures were mixed for 7 min with a 70-l rotating planetary mixer. After the mixing procedure was completed, tests were conducted on fresh concrete to determine slump flow diameter and V-funnel flow time. The results of fresh concrete tests are also shown in Table 2. As seen in that table, the slump flow diameters of all mixtures were in the range of 640–670 mm, and the V-funnel flow times were in the range of 10.3–15.4 s. In addition to the above properties, visual inspection of fresh concrete did not detect any segregation or bleeding in any of the mixtures during the slump flow test. Therefore, all concrete mixtures were considered as SCC in accordance with EFNARC [26]. Also observed in Table 2, is the change in SP content for the same workability measure. The control mixture (without FA) had the highest SP content, but as part of the PC was replaced by FA, the SP content of mixtures decreased. The smooth surface characteristics and spherical shape of the FA (Fig. 2) improved the workability characteristics of concrete mixtures, and similar workability properties were achieved by using a lower SP content.

From each concrete mixture, Ø100 × 200-mm cylinder specimens were prepared for the determination of compressive strength and permeation tests. All specimens were cast in one layer without any compaction. At the age of 24 h, the specimens were removed from the molds and stored in lime-saturated water at 23 ± 2 °C for 28 days.

Generally, microcracking steadily increases with applied compressive loading. Bond cracking is shown to be predominant in the early phases of loading while mortar cracks become abundant near failure [27]. The permeation properties of concrete are not usually affected from the bond cracking. Hence, an abundance of load-induced microcracks alone does not necessarily increase the rate at which substances move through the concrete. It is only when the cracks begin to interconnect that change in mass transport and liquid flow can be expected to occur [27]. At low levels of applied load, most of the cracks are formed at discrete locations, where the stress concentration is the highest and primarily at the aggregate–paste interface. Mortar cracking increases only at higher loads and near failure. In general, it was found out that load-induced microcracks do not lead to an increase in permeability and loss in compressive strength up to a load level of about 70% of maximum strength [28]. Therefore, after 28 days of moist curing, the compressive strength of each mixture was determined, and the remaining specimens were pre-loaded to 0%, 70% and 90% of their corresponding compressive strength. When the compressive strength reached the required pre-determined strength value, the load was released. Later, the pre-loaded specimens are further stored in lime-saturated water at 23 ± 2 °C for an additional 30 days.

For this experimental program, tests performed on hardened concrete can be grouped into two; tests to determine the mechanical properties and tests to determine the permeation properties. As for the mechanical properties, the compressive strength and ultrasonic pulse velocity (UPV) of the concrete specimens were determined at 28, 28 + 15 and 28 + 30 days by using three specimens at each age. The permeation properties were also determined at 28, 28 + 15 and 28 + 30 days, using both the sorptivity and rapid chloride permeability (RCPT) tests in accordance with the ASTM C1585 and ASTM C1202 specifications, respectively. For the permeation properties of pre-cracked concrete specimens, cylinders were sawed into 50 mm thick slices and the two middle slices from each specimen were used for testing.

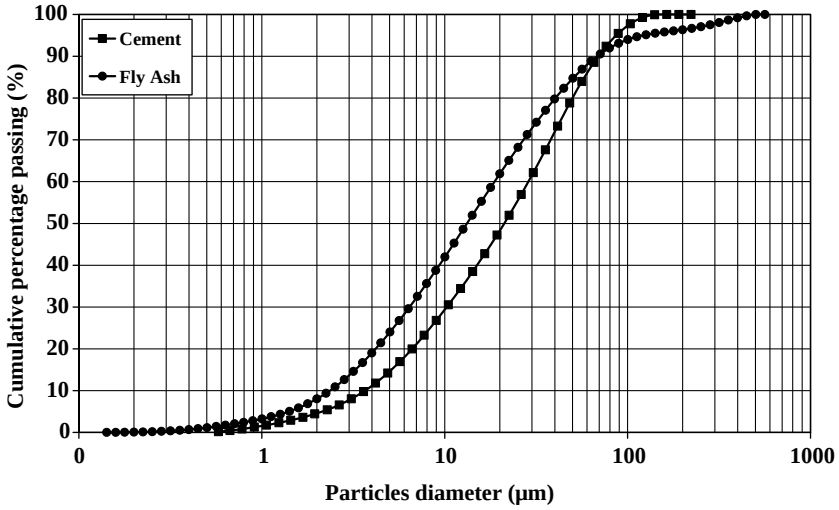

Fig. 1. Particle size distribution of Portland cement and fly ash.

Table 2
SCC mixture proportions

Mix ID	W/B[a]	Ingredient (kg/m^3)						Fresh properties	
		Water	PC	FA	Aggregate		SP	Slump flow (mm)	V-funnel flow time (s)
					Fine	Coarse			
Control	0.35	175	500	0	888	888	7.4	660	15.4
F_35	0.35	175	325	175	858	858	6.7	670	10.3
F_55	0.35	175	225	275	841	841	5.9	640	11.2

[a] B: Binder (PC + FA).

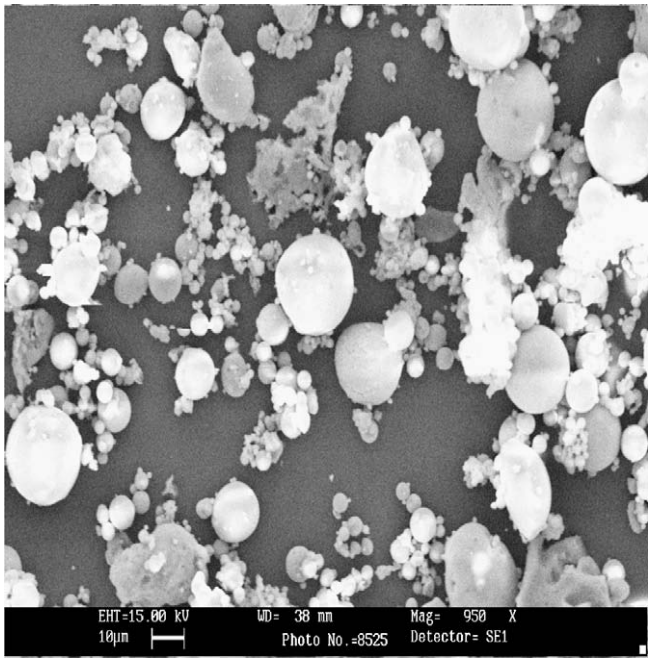

Fig. 2. Secondary electron images of the fly ash showing their particle morphology.

The two test procedures used to measure permeation properties, rapid chloride permeability and sorptivity test, predicted different performance of concrete. The sorptivity test method is used to determine the rate of sorptivity of water by concrete by measuring the increase in the mass of a pre-dried specimen resulting from absorption of water as a function of time, when only one surface of the specimen is exposed to water [29]. The exposed surface of the specimen is immersed in water and water ingress of unsaturated concrete dominated by capillary suction during initial contact with water. On the other hand, rapid chloride permeability test (RCPT) is a measure of the concrete's resistivity – an indirect measure of chloride penetrability [30]. However, RCPT is a simple index of chloride permeability which is reported to correlate with the 90-day ponding test described by AASHTO T259 [31].

2.3. Sorptivity test

The sorptivity test was based on ASTM C1585 [29]. The sorptivity test consisted of registering the increase in mass of a prism specimen (Ø100 × 50 mm) at given intervals of time (1, 2, 3, 4, 6, 8, 12, 16, 20, 25, 36, 49, 64, 81, 120 and 360 min) when permitted to absorb water by capillary suction. The specimens were dried in an oven at 50 ± 5 °C for three days. Only one surface of the specimen was allowed to be in contact with water, with the depth of water between 3 and 5 mm (Fig. 3). The sides of the specimen were sealed with a silicone coating in order to have one-directional flow through the specimen. The rate of absorption (mm), defined as the change in mass (g) divided by the cross sectional area of the test specimen (mm^2) and the density of water at the recorded temperature (g/mm^3), was plotted against square root of time (min$^{1/2}$). The slope of the obtained line defines the sorptivity index (S_0) of the specimen during the initial 6 h of testing. For all specimens, this slope is obtained by using least-squares, linear regression analysis of the plot of the rate of absorption versus the square root of time. This test was chosen as it measures the rate of ingress of water through unsaturated concrete.

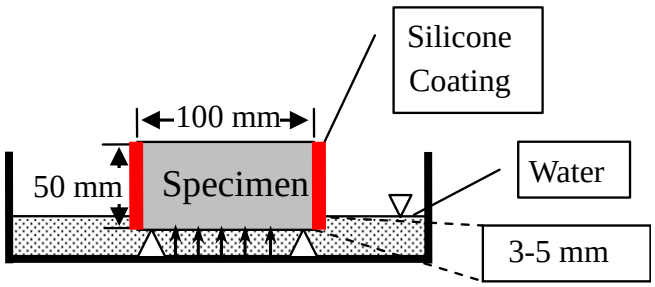

Fig. 3. Schematic diagram of sorptivity test.

2.4. Rapid chloride permeability test (RCPT)

This test was based on the ASTM C1202 [30] for determining the chloride permeability of hardened concrete. In this test, a water saturated 50 mm thick, 100 mm diameter concrete specimen was subjected to a 60 V applied DC voltage for 6 h. One end of the specimen is in contact with 0.3 M NaOH solution, the other end with 3.0% NaCl solution. The total charge passed during 6 h is then determined. The total charge passed, in coulombs, is related to the concrete's ability to resist chloride ion penetration. As more chloride ions migrate into the concrete, more current can pass through, and the total charge passed during 6 h increases. A high value for total charge passed indicates that the concrete is highly penetrable.

3. Results and discussion

3.1. Unhealed specimens

Table 3 presents the mechanical and permeation properties of concrete specimens at 28 days that were previously pre-loaded to 70% or 90% of their compressive strength. As these specimens were tested immediately after the release of pre-loading, they had no time to undergo any crack healing. Properties of virgin (pre-load level of 0%) specimens are also included in this table.

The results revealed that for specimens that are not pre-loaded, the compressive strength and ultrasonic pulse velocity were affected by FA replacement. As the FA replacement ratio was increased to 55% there was a more noticeable reduction in the mechanical properties, especially the compressive strength. As for the permeation properties, despite its higher compressive strength, undamaged control specimens had an average charge passed of 4444 coulomb and average sorptivity index of 0.113 mm/min$^{1/2}$, which are significantly higher than those of SCC mixtures with FA. It, therefore, appears that the control mixture (mixture without FA) was more permeable than the SCC containing FA. The effect of FA on the permeation properties of concretes was also studied by other researchers. For example, Shi stated that the use of supplementary cementitious materials such as FA may have a significant effect on the permeability of concrete as measured by the RCPT [32]. The use of FA, even though it causes lower compressive strength especially at earlier ages, generally, improves the permeation properties of concrete by producing a denser concrete, by reducing the pore sizes and microcracking in the transition zone [33]. On the other hand, an increase in FA content from 35% to 55% showed no significant effect on permeation properties.

Table 3
Mechanical and permeation properties of unhealed specimens

Fly ash (%)	Pre-load level		
	0%	70%	90%
Compressive strength, f'_c (MPa)			
0	51.3	48.3	41.3
35	46.4	43.1	35.6
55	38.7	33.4	28.1
Ultrasonic pulse velocity, UPV (m/s)			
0	4864	4767	4618
35	4932	4810	4698
55	4886	4701	4430
Rapid chloride permeability, RCPT (coulombs)			
0	4444	5106	6229
35	1385	1835	2307
55	1542	2207	2675
Sorptivity index, S_0 (mm/min$^{1/2}$)			
0	0.113	0.141	0.177
35	0.084	0.122	0.151
55	0.089	0.129	0.162

A typical plot of the cumulative water absorption (normalized per unit surface area) as a function of the square root of time is shown in Fig. 4. It can be seen that the cumulative volume of water absorbed per unit surface area (mm^3/mm^2) in the specimens increased with the square root of time. The presence of microcracking in concrete significantly alters the transport properties measured as a function of the pre-loading level. The water absorption rate is high when the pre-loading level applied on the specimens increases. In particular, for the highly damaged concrete specimen, the initial rate of water absorption (up to 36 min) was very high thereby implying that the cracks and capillary pores were saturated in a very short time. It was also observed from Fig. 4 that for the highly damaged concrete specimens (e.g. pre-loading level = 90%), the cumulative water absorption increased nonlinearly with the square root of time. The highest nonlinearity was obtained from the FA_55 specimens pre-loaded to 90% of their compressive strength, and the minimum coefficient of correlation value of 0.94 (from linear regression) was observed for these specimens. The nonlinearity for the microcracked SCC specimens was likely due to the fact that the capillary absorption into the crack system is quite weak and reaches capillary rise equilibrium against gravity in the course of the test [34]. In the case of cracked specimens, therefore, the observed cumulative absorption arises from the combination of two processes: the absorption into the uncracked matrix where the capillary forces are strong compared with the opposing gravitational forces; while the absorption into the crack system reaches a limiting equilibrium value. Another reason of nonlinearity may be attributed to the fact that the water may rapidly fill the microcracks due to the large capillary suction forces and absorption may also occur from the crack surfaces, and thus, the cross sectional area of the specimen used for the calculation of water front is incorrect. This indicates that microcracks induced by mechanical loading facilitated the water ingress in concrete.

In order to visualize the extent of damage on the properties of all mixtures, for each property measured the percent change in the measured parameter is determined against pre-loading level in Fig. 5. As seen from this figure, there was a reduction in the mechanical properties and there was an increase in the permeation properties. It can also be observed from Fig. 5 that the permeation properties are much more affected from the pre-loading than the mechanical properties. For example, at 90% pre-load level, the highest effects were observed in the sorptivity index, S_0, which exhibited an 82% increase when compared to that of the virgin specimens. Moreover, it should also be mentioned that when the FA is used in the production of SCC, the reduction in mechanical properties and increase in permeation properties are more influenced from the mechanical pre-loading. For example, as seen from Fig. 5, a 15% increase in RCPT was observed when control specimens were loaded to 70% of their ultimate load. This difference

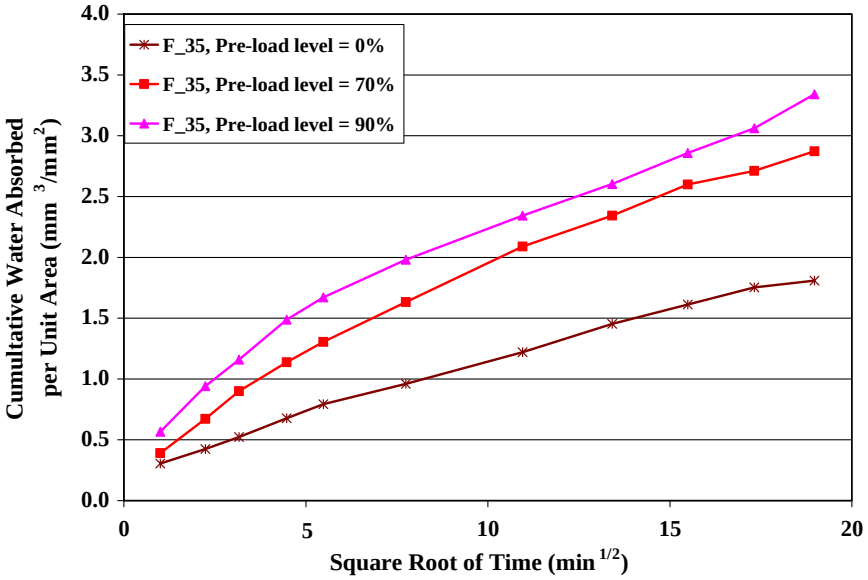

Fig. 4. Typical plot of the sorptivity test.

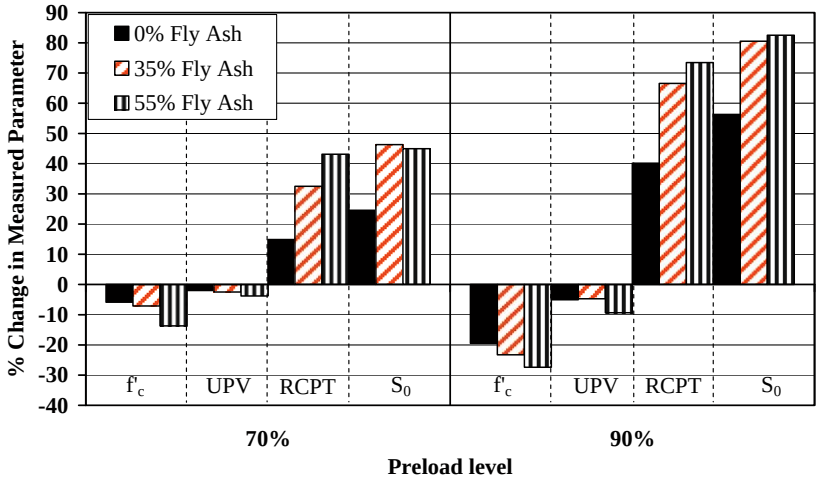

Fig. 5. Change in mechanical and permeation properties for unhealed specimens.

rose to a 40% increase in RCPT at 90% pre-load level. On the other hand, the average increase in RCPT for SCC mixtures with FA varied from 40% to about 73% between virgin and specimens pre-loaded to 90%. Similar trends were also observed for the sorptivity test results of SCC mixtures with FA. Therefore, it could be stated that the properties of newly damaged HVFA–SCC specimens are more affected from the mechanical pre-loading than the control SCC specimens. This may be attributed to the fact that an increase in the FA content caused a reduction in the compressive strength and a weaker paste–aggregate interfacial transition zone at the age of the pre-loading.

As pointed above, in this study loading concrete specimens even up to 70% of the ultimate load considerably influenced the strength and permeation properties of the specimens when compared to the virgin specimens. This may seem to be in disagreement with literature [28,35]. However, in those studies the rate of loading was maintained as specified by ASTM standards for testing the specimens in compression. In this study, however, the rate of loading was kept constant at 0.06 MPa/s, and this rate of loading level was significantly lower than that of specified by ASTM C39 standard (0.15–0.35 MPa/s) [36]. Therefore, this disagreement is attributed to the differences in loading rate, as it has been known that the extent of damage into the internal structure of loaded specimens is largely depended on how long the applied load was maintained on the specimens during the compressive test [28].

3.2. Effects of self-healing

Table 4 presents the results of compressive strength, UPV, RCPT and sorptivity tests from specimens that were subjected to pre-loading and later stored up to 30 days in water in order to evaluate the extent of self-healing.

For the virgin specimens, when the test results after 28 days are considered (Tables 3 and 4), it could be seen that there is a steady increase in the mechanical properties and a reduction in the permeation properties. Therefore, comparing the properties of pre-loaded specimens by age will not necessarily point out any self-healing, as the hydration reactions continue even in the undamaged specimens.

Table 4
Mechanical and permeation properties of self-healed specimens

Fly ash (%)	After 15 days of self-healing			After 30 days of self-healing		
	Pre-load level			Pre-load level		
	0%	70%	90%	0%	70%	90%
Compressive strength, f'_c (MPa)						
0	53.3	53.5	45.9	55.8	56.9	48.3
35	56.8	51.3	49.8	62.8	57.1	56.3
55	46.5	43.4	40.2	51.8	50.2	48.1
Ultrasonic pulse velocity, UPV (m/s)						
0	4911	4810	4721	4950	4916	4887
35	4980	4901	4853	5006	4986	4910
55	4954	4887	4793	4948	4945	4875
Rapid chloride permeability, RCPT (coulombs)						
0	3440	4440	5235	3421	3921	4640
35	1150	1282	1574	910	970	1170
55	1275	1386	1555	870	945	1046
Sorptivity index, S_0 (mm/min$^{1/2}$)						
0	[a]	0.118	0.139	0.102	0.108	0.120
35	[a]	0.097	0.105	0.056	0.067	0.078
55	[a]	0.099	0.112	0.050	0.055	0.075

[a] Test could not be conducted for this series due to lack of specimens.

For this reason, the extent of any self-healing could be best detected, by comparing the results of pre-loaded and virgin specimens' properties at a particular age. As seen from Tables 3 and 4, the measurable damage and healing were the least clear with the ultrasonic pulse velocity and the most clear with the RCPT.

By comparing the plot of the cumulative water absorption of healed specimens stored in water with that shown for the mechanically pre-loaded specimens before exposure in Fig. 4, it can be observed that a significant reduction of the nonlinearity of cumulative water absorption with the square root of time has been observed even after 15 days moist curing period. The minimum coefficient of correlation value of 0.98 (from linear regression) was observed for the healed specimens. This suggests that between the time of inducing pre-cracking and the time of testing, after immersion in lime-saturated water, healing of the microcracks has occurred in the SCC specimens.

In order to draw a clearer picture only the compressive strength and RCPT results are presented in Fig. 6 and the following discussions are based on compressive strength as for the most clear mechanical property, and RCPT as for the most clear permeation property.

As presented in Fig. 6a, for the control SCC mixture (with 0% FA) that did not go through any healing, pre-loading up to 70% caused a strength reduction of about 6%. However, as observed in Fig. 6b and c, with subsequent curing in water, the strength reduction vanished even after 15 days of moist curing. For the same mixture, when the amount of pre-loading was increased to 90%, the amount of strength reduction came down from 19% to about 14% in the first 15 days, and later to 13% in the next 15 days. These amounts of reduction, demonstrate the extent of self-healing on the control mixture as detected by its strength. When the HVFA–SCC mixtures are examined, for a FA replacement level of 35%, the compressive strength reduction due to a pre-loading of 90% was 23% at 28 days and with subsequent curing reduced to 12% in the first 15 days, and later to 10% in the next 15 days. As the FA replacement level increased up to 55%, the compressive strength reductions were more visible. For 90% of pre-loading, the reduction amount reduced from 27% to 14% in the first 15 days, and later to 7% in the next 15 days. From the above mentioned discussions, it was observed that although the reduction in compressive strength of control SCC mixture after pre-loading is less than that of SCC mixtures with FA, the unhydrated cementitious material available for further hydration is also lower. Therefore, it appears that the FA significantly influences the self-healing of the mechanically pre-loaded specimens even after 15 days moist curing. The C–S–H gels formed through pozzolanic reactions developed a good bond within the microcracks. Similar conclusions could also be made for UPV. However, it could be stated that among the mechanical properties, the effects of self-healing can better be shown on strength rather than UPV. As the specimens were tested when they are fully saturated, the effects of humidity were clearer on strength. However, the moisture in the cracks hindered the reduction in UPV [37,38].

As presented earlier in Table 3, pre-loading causes microcracks, which effectively increase the overall porosity and permeability of the system. The effects of self-healing on the permeation properties of SCC mixtures pre-loaded to a level of 70% and 90% could again be followed by examining the test data presented in Table 4. The effects of self-healing are more visible on the permeation properties when compared to the mechanical properties. Therefore, by looking at the RCPT increase presented in Fig. 6a, it could be observed that for the control SCC pre-loaded up to 70%, the increase in RCPT was 15% at 28 days, and with 30 days of subsequent curing it remained about the same. For the control SCC specimens pre-loaded up to 90%, the increase in RCPT was 40% at 28 days, and with 30 days of subsequent curing it remained about 36%. Similar observations could also be made for the permeation properties as determined by the sorptivity index. When the HVFA–SCC mixtures are examined, for a FA replacement level of 35%, the increase in RCPT due to a pre-loading of 70% dropped down from 32% to 11% after a curing period of 15 days, and later to 7% in the next 15 days. For 90% of pre-loading, however, the reduction amount reduced from 67% to 37% in the first 15 days, and later to 29% in the next 15 days.

From the present study, self-healing of microcracks of HVFA–SCC under water is evident from the mechanical and permeation properties previously discussed. The mechanical and permeation properties indicate that microcracks of HVFA–SCC exposed to water showed significant self-healing in 30 days. This can be attributed primarily to the high cementitious material content and relatively low water to binder ratio within the HVFA–SCC mixture. As a result of the formation of microcracks due to mechanical loading, unhydrated cementitious particles (unhydrated fly ash) are easily exposed to the water, which leads to development of further hydration processes. Therefore, in addition to water, the other essential requirement for self-healing process is the presence of compounds capable of further reaction,

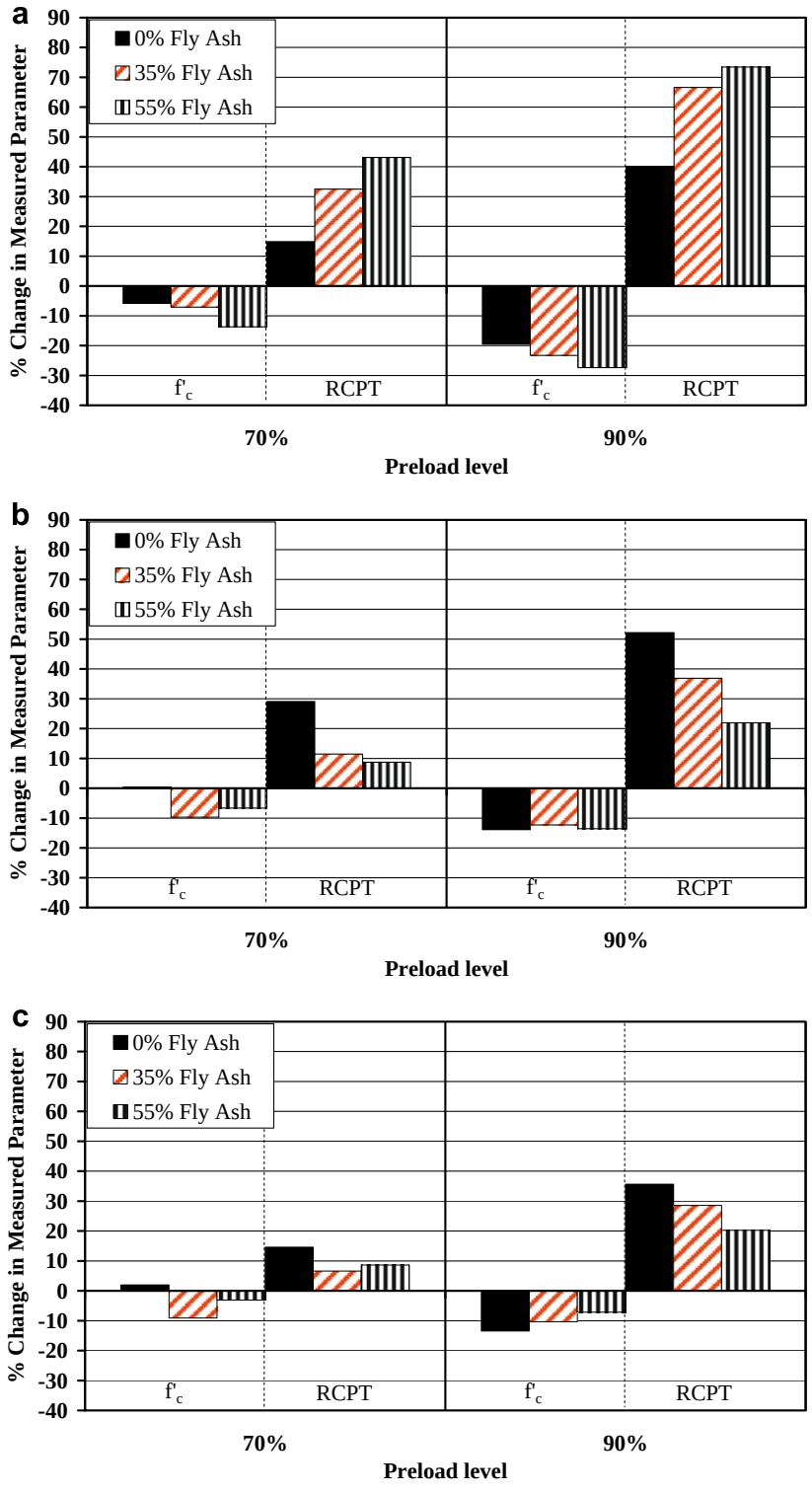

Fig. 6. Change in strength (f'_c) and permeability (RCPT) of self-healed specimens: (a) before any healing, (b) after 15 days of healing, (c) after 30 days of healing.

such as unhydrated FA particles. When these requirements are available, the structures where the self-healing may be beneficial are culverts, piles, pipes, tunnels, water reservoirs, basements, water retaining structures, pavements and marine structures. Finally microcracks under conditions of a damp environment were closed by newly formed products, which can also reduce the ingress of aggressive ions when compared to the unhealed specimens.

4. Conclusions

In this article, the results of an experimental investigation on the mechanical and permeation properties of self-healed SCC specimens are presented. After a controlled pre-cracking phase up to 90% of the ultimate compressive strength, specimens are cured in water for an additional 30 days. Pre-loading the concrete caused an increase in its total porosity and a loss in its ultimate compressive

strength. As microcracks developed inside the concrete structure, the pore structure was modified and the continuity of the cracks was increased.

Internal cracking due to the mechanical loading initially reduced the compressive strength by about 6–27%, and increased the average charge passed by 15–73%. Then the specimens were stored in water for an additional month. It was observed that HVFA–SCC mixtures initially lost 27% of their strength when preloaded up to 90% of their ultimate strength, and after 30 days of water curing that reduction was only 7% with respect to virgin specimens at the same age, indicating a substantial healing. On the other hand, for SCC specimens without FA that were pre-loaded to the same level, the loss in strength was initially 19% and after a month it was only 13%. Similar observations were also made on the permeation properties with greater effects. This was explained to be due to the fact that the HVFA–SCCs studied have an important amount of unhydrated FA particles available in its microstructure, and these observations are attributed to the self-healing of the pre-existing crack, mainly by hydration of anhydrous FA on the crack surfaces. Recovery of compressive strength and permeation properties can be related to the progressive filling of the crack by newly formed C–S–H gels due to the pozzolanic reactions.

References

[1] Oh BH, Cha SW, Jang BS, Jang SY. Development of high-performance concrete having high resistance to chloride penetration. Nucl Eng Des 2002;212(1–3):221–31.

[2] Beeldens A, Vandewalle L. Durability of high strength concrete for highway pavement restoration. In: Proceedings of CONSEC '01: third international conference on concrete under severe conditions. Vancouver, Canada; 2001. p. 1230–8.

[3] Hwang CL, Liu JJ, Lee LS, Lin FY. Densified mixture design algorithm and early properties of high performance concrete. Journal of the Chinese Institute of Civil and Hydraulic Engineering 1996;8(2):217–29.

[4] Chang PK, Peng YN, Hwang CL. A design consideration for durability of high-performance concrete. Cem Concr Compos 2001;23(4–5):375–80.

[5] Mehta PK. Concrete: structure, properties, and materials. Englewood Cliffs, New Jersey: Prentice-Hall; 1986.

[6] Mora J, Aguado A, Gettu R. The influence of shrinkage reducing admixtures on plastic shrinkage. Mater Constrc 2003;53(271–272):71–80.

[7] Weiss WJ, Shah SP. Restrained shrinkage cracking: the role of shrinkage reducing admixtures and specimen geometry. Mater Struct 2002;35(246):85–91.

[8] Mihashi H, De Leite JPB. State-of-the-art report on control of cracking in early age concrete. J Adv Concr Technol 2004;2(2):141–54.

[9] TRB Basic Research and Emerging Concrete Technologies Committee. Control of cracking-state of the art, transportation research circular E-C107. Washington DC: Transportation Research Board; 2006.

[10] Ozawa K, Maekawa K, Kunishima M, Okamura H. Development of high performance concrete based on the durability design of concrete structures. In Proceedings of the second East-Asia and Pacific conference on structural engineering and construction (EASEC-2). Tokyo, Japan; 1989. p. 445–50.

[11] Okamura H, Ouchi M. Self compacting concrete.J Adv Concr Technol 2003;1(1):5–15.

[12] Nehdi M, Pardhan M, Koshowski S. Durability of self-consolidating concrete incorporating high-volume replacement composite cements. Cem Concr Res 2004;34(11):2103–12.

[13] Leemann A, Hoffmann C. Properties of self-compacting concrete and conventional concrete – differences and similarities. Mag Concr Res 2005;57(6):315–9.

[14] Bouzoubaa N, Lachemi M. Self-compacting concrete incorporating high volumes of class F fly ash preliminary results. Cem Concr Res 2001;31(3):413–20.

[15] Şahmaran M, Yaman İÖ, Tokyay M. Development of high volume low-lime and high-lime fly-ash-incorporated self consolidating concrete. Mag Concr Res 2007;59(2):97–106.

[16] Powers TC, Copeland LE, Hayes JC, Mann HM. Permeability of Portland cement paste. ACI J Proc 1954;51(3):285–98.

[17] Hearn N, Morley CT. Self-sealing property of concrete – experimental evidence. Mater Struct 1997;30(201):404–11.

[18] Jacobsen S, Sellevold E. Self-healing of high strength concrete after deterioration by freeze/thaw. Cem Concr Res 1996;26(1):55–62.

[19] Jacobsen S, Marchand JJ, Hornain H. Sem observations of the microstructure of frost deteriorated and self-healed concrete. Cem Concr Res 1995;25(8):55–62.

[20] Abrams D. Autogeneous healing of concrete. Concrete 1925;27(2):50.

[21] Clear CA. The effects of autogenous healing upon the leakage of water through cracks in concrete. Cement and Concrete Association, London UK Technical Report 559 1985.

[22] Munday JCL, Sangha CM, Dhir RK. Comparative study of autogeneous healing of different concretes. In Proceedings of first australian conference on engineering materials. Sydney, Australia; 1974. p. 177–89.

[23] Edvardsen C. Water permeability and autogenous healing of cracks in concrete. ACI Mater J 1999;96(4):448–54.

[24] Reinhardt HW, Joos M. Permeability and self-healing of cracked concrete as a function of temperature and crack width. Cem Concr Res 2003;33(7):981–5.

[25] TS EN 197-1. Part 1: Cement: compositions and conformity criteria for common cements. TSE, Ankara: Turkish Standards Institution; 2004.

[26] EFNARC. Specification and guidelines for self-compacting concrete. English ed. Norfolk, UK: European Federation for Specialist Construction Chemicals and Concrete Systems; 2002.

[27] Hearn N. Effect of shrinkage and load-induced cracking on water permeability of concrete. ACI Mater J 1999;96(2):234–41.

[28] Samaha HR, Hover KC. Influence of microcracking on the mass transport properties of concrete. ACI Mater J 1992;89(4):416–24.

[29] ASTM C1585. Standard test method for measurement of rate of absorption of water by hydraulic-cement concretes. West Conshohocken, PA: American Society for Testing and Materials; 2004.

[30] ASTM C1202. Standard test method for electrical indication of concrete's ability to resist chloride ion penetration. West Conshohocken, PA: American Society for Testing and Materials; 2002.

[31] Whiting D. Permeability of selected concretes. Permeability Concr ACI SP 1998;108–111:195–222.

[32] Shi C. Effect of mixing proportions of concrete on its electrical conductivity and rapid chloride permeability test results. Cem Concr Res 2004;34(3):537–45.

[33] Mehta PK, Monteiro PJM. Concrete – microstructure, properties, and materials. 3rd ed. New York: Mc Graw Hill; 2006.

[34] Hall C, Hoff WD. Water transport in brick, stone and concrete. London and New York: Spon; 2002.

[35] Abdel-Jawad Y, Haddad R. Effect of early overloading of concrete on strength at later ages. Cem Concr Res 1992;22(5):927–36.

[36] ASTM C39. Standard test method for compressive strength of cylindrical concrete specimens. West Conshohocken, PA: American Society for Testing and Materials; 1999.

[37] Yaman IO, Hearn N, Aktan HM. Active and non-active porosity in concrete part I: experimental evidence. Mater Struct 2002;35(3):102–9.

[38] Yaman IO, Hearn N, Aktan HM. Active and non-active porosity in concrete part II: evaluation of existing models. Mater Struct 2002;35(3):110–6.